Shiraz University

IJVR

ISSN: 1728-1997 (Print)
ISSN: 2252-0589 (Online)

Vol. 22 No. 4 Ser. No. 77 2021

IRANIAN JOURNAL OF VETERINARY RESEARCH

Original Article

Morphology of the lips, cheeks, and the hard palate of the Egyptian water buffalo (*Bubalus bubalis*): a focus on histological, histochemical, and ultrastructural aspects

Farrag, F. A.[1]; Morsy, K.[2]; Hamdi, H.[3]; Kassab, M.[4]; Hassan, A.[1]; Abdelmohdy, F.[4]; Shukry, M.[5]; Abumandour, M. M. A.[6*] and Fayed, M.[1]

[1]Department of Anatomy and Embryology, Faculty of Veterinary Medicine, Kafrelsheikh University, 33511 Kafrelsheikh, Egypt; [2]Biology Department, College of Science, King Khalid University, Abha, Saudi Arabia, and Zoology Department, Faculty of Science, Cairo University, Cairo, Egypt; [3]Biology Department, College of Science, Taif University, Taif, Saudi Arabia; [4]Department of Cytology and Histology, Faculty of Veterinary Medicine, Kafrelsheikh University, 33511 Kafrelsheikh, Egypt, [5]Department of Physiology, Faculty of Veterinary Medicine, Kafrelsheikh University, 33511 Kafrelsheikh, Egypt; [6]Department of Anatomy and Embryology, Faculty of Veterinary Medicine, Alexandria University, Alexandria, Egypt (current address)

[*]***Correspondence:*** *M. M. A. Abumandour, Department of Anatomy and Embryology, Faculty of Veterinary Medicine, Alexandria University, Alexandria, Egypt (current address). E-mail: M.abumandour@alexu.edu.eg*

10.22099/IJVR.2021.40728.5898

(Received 21 May 2021; revised version 29 Sept 2021; accepted 17 Oct 2021)

Abstract

Background: The available data is scanty about Egyptian water buffalo lips, cheeks, and palate. **Aims:** The current investigation was focused on describing the morphology of the lip, cheek, and palate. **Methods:** Our study included the gross, light, and electron microscopic examinations of ten heads of the Egyptian water buffalos. **Results:** The nasolabial plate surface carried numerous scales of keratinized epithelium. Internal labial surface and labial mucocutaneous junctions were covered with stratified squamous keratinized epithelium. Two types of hair follicles in the dermis included ordinary and cavernous types characterized by cavernous space. The conical papillae on the internal aspect of the oral commissure were projected from the mucous membrane. Seromucous glands were occasionally observed under the oral mucous membrane of the commissure and gave positive PAS and AB. Conical papillae density on the inner cheek surface had some variations: the rostral part had large papillae, while the dorsal part had numerous papillae than the ventral part, the caudal part had a smaller number of papillae, while the middle part was devoid of papillae. Parotid duct opening in the buccal vestibule was without papillae. Conical papillae had two surfaces; the rostral surface was highly keratinized than the caudal one. The buccal gland was a compound tubuloacinar mixed (mucoserous) gland and mucus acini only reacted to PAS and AB. The oral surface of palatine rugae was covered with highly keratinized epithelium than the aboral surface. Palatine glands showed PAS and AB positive. **Conclusion:** The result describes the relationship between the available food particles, environmental conditions and the lip, cheek, and palate appearance, and structure.

Key words: Cheek, Lip, Egyptian water buffalo, Histology, Scanning electron microscope

Introduction

The Egyptian water buffalo (*Bubalus bubalis*) belongs to the order *Artiodactyla*, suborder *Ruminantia*, family *Bovidae*, genus *Bubalus*, species *B. bubalis* (Linnaeus, 1758). The Egyptian water buffalo is considered the most important domestic ruminants in Egypt, and reached about 4 million heads (FAO, 2013). The large ruminants, including the Egyptian water buffalo, eat grass and other roughage by utilizing their lips and tongues to choose portions of the plant that are simpler to process or higher in sustenance (Maala *et al*., 2007), by helping variable quantities of material hairs and standard fine hairs which covered the labial skin (Baumel, 1975).

Ingestive instruments fluctuate altogether among various animal species mirroring their dietary propensity, eating, and anatomic structures of the oral cavity and digestive tract. The main factor that influences the productive performance of the animal is its healthy behavior (Klein *et al*., 2021). The previously published data of the ruminants have concerned on the lingual characterizations to describe their feeding behaviors (El-Bakary and Abumandour, 2017), while recently some published articles try to relate the feeding behaviors of ruminant species with the morphological characterizations of the lips and cheek (Mahdy *et al*., 2020; Madkour and Mohammed, 2021). Still, the hard palate and its role in the collection, manipulation, and mastication of the food particles had little interest.

The movable lips of equine, and ruminants are utilized for selecting an assortment of nourishments but fixed lips are in canine for catching the food particles (König and Liebich, 2013). The lips with the cheek form

the rostral and lateral walls of the oral cavity vestibule (Nickel *et al*., 1986). In addition to its role in food selection and collection, the lips help a mechanical role in the first down of the collected food particles (Bone, 1979). Also, it had a tactile function that appear in the process of suckling and food selection (König and Liebich, 2013). Moreover, the cheeks help manipulate the collected food particles inside the oral cavity and hold the food set up while the teeth cut it (Seeley *et al*., 2006). The lips, cheek, and palate of the equine, ruminates, camel, and dog were previously described (Getty, 1975; Nickel *et al*., 1986; Budras *et al*., 2003; Dyce *et al*., 2010; König and Liebich, 2013). Recently, some published articles described the morphological appearance of the lips and cheeks of sheep, goats (Mahdy *et al*., 2020; Madkour and Mohammed, 2021), and Alpaca (Gozdziewska-Harłajczuk *et al*., 2015).

The available data about the Egyptian water buffalo's (*B. bubalis*) lips, cheek, and palate is limited. So, the present work was designed to provide a complete morphological description of the lips, cheek, and the palate of the Egyptian water buffalo (*B. bubalis*) using the gross, scanning electron microscope, and histological techniques to relate these characteristic features with the feeding strategic of Egyptian water buffalo (*B. bubalis*). The findings were compared to those described in the previously published data on the ruminant and other domesticated animal species.

Materials and Methods

Animal samples collection

Ten heads from the normal healthy adult Egyptian water buffalo (*B. bubalis*) of both sexes (5 males and 5 females) aged 1.5 years were collected in spring from the local slaughterhouse in Kafrelsheikh Governate, Egypt. The examined samples were directly collected after slaughtering.

The current work was done according to the guidelines for the using and caring of the laboratory animals and following the animal Ethics and welfare in the Faculty of Veterinary Medicine, Alexandria University, and according to the Egyptian's laws.

Gross morphology observations

The lips (upper and lower), cheek, and hard palate were collected from four Egyptian water buffalo heads of both sexes and were used to demonstrate the gross anatomical appearance and position of the lip, cheek, and hard palate. Then, the collected samples were fixed in 10% formalin. The gross anatomical images were photographed by a digital camera (Canon IXY 325, Japan).

Histological and histochemistry studies

Three Egyptian water buffalo (*B. bubalis*) heads were selected out of the four heads and the lips (upper and lower), cheeks, and hard palates were studied via the histological technique under a light microscope in a new state according to the previous study (Suvarna *et al*., 2013). The collected samples (lips, cheek, and hard palate) were fixed in 10% neutral buffer formalin. After 24-48 h, the samples were gently transferred to 70% alcohol and dehydrated in ascending graded series of ethanol. The samples were cleared in xylene and impregnated and embedded in paraffin wax. Sections of 5-7 µm were cut using Leica rotatory microtome (RM 20352035; Leica Microsystems, Wetzlar, Germany) and mounted on glass slides. Paraffin sections were used for conventional staining (H&E) for general histological examinations (Bancroft and Gamble, 2008).

For histochemistry processing, the sections were stained with the Periodic Acid-Schiff technique (PAS) (ab150680) to demonstrate the neutral mucin (Schumacher *et al*., 2004), Alcian Blue (AB) at a pH of 2.5 (ab150662) for acidic mucin (Bancroft *et al*., 1996; Suvarna *et al*., 2018), Van Gieson (mixture of picric acid and acid fuchsin) for elastic fibers in connective tissue, trichrome for collagen fibers in the connective tissue (Masson, 1929). The stained sections were examined with a BX50/BXFLA microscope (Olympus, Tokyo, Japan) according to Suvarna *et al*. (2013).

Scanning electron microscopy (SEM)

Three Egyptian water buffalo (*B. bubalis*) heads were used to collect the samples (lips, cheek, and hard palate). The collected samples were prepared for the SEM technique (Abumandour and El-Bakary, 2013; Abumandour, 2018). The samples (lips, cheek, and hard palate) were fixed at 4°C in a solution of fixation formed from; 2% formaldehyde, 1.25% glutaraldehyde in 0.1 M sodium cacodylate buffer, pH = 7.2. Once fixation occurs, the collected samples (lips, cheek, and hard palate) were washed in 0.1 M sodium cacodylate containing 5% sucrose, processed through tannic acid. Finally, the lingual samples were dehydrated by increasing the ethanol concentration (15 min each in 50, 70, 80, 90, 95, and 100% ethanol). The collected samples (lips, cheek, and hard palate) were then dried in carbon dioxide and attached to stubs with colloidal carbon and coated with gold-palladium in a sputtering device. Finally, the collected samples were examined and photographed with a JEOL scanning electron microscope operating at 15 kV, at the Faculty of Science, Alexandria University.

Results

Lips

Gross and SEM morphological appearance of the lips

The partially movable hard texture lips of the Egyptian water buffalo were joined together laterally at the semicircular oral angle and the oral labial commissure. The upper lip was larger, longer, thicker, and more movable than the lower lip (Figs. 1A-C and 2A). The external labial surface had a rough skin with many long ordinary hairs and tactile hairs were depressed in their origins (Figs. 3A-C). Moreover, the tactile hairs were mainly observed on the free border of the upper and lower lips, but their numbers were more in

the upper lip than the lower lip, while the longer tactile hairs were observed in the lower lip. The number of tactile hairs was decreased toward the oral labial commissure. The mucosa of each lip was reflected on the alveolar border rather than on the dental pad of the upper lip forming the frenulum labii (Figs. 2A and 4A).

The free movable border of the upper and lower lips carried numerous blunt short papillae (Fig. 2A). The SEM observations separated these papillae by narrow fissures that crossed each other (Fig. 2B). At a high SEM

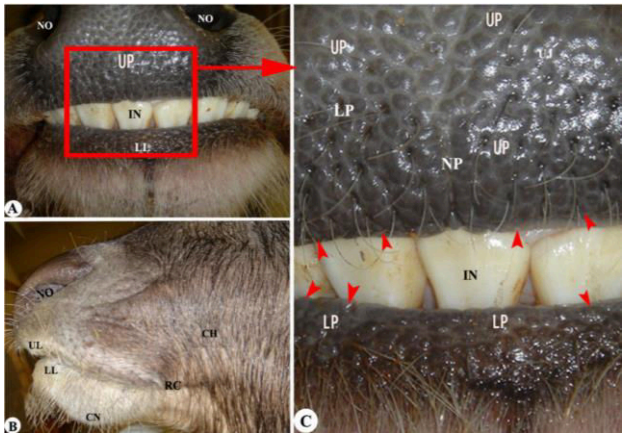

Fig. 1: Gross anatomical images (**A**, **B**, and **C**) of the external appearance of the lips and cheek of the Egyptian water buffalo to show the upper lip (UL) with projections (ULP), and nasolabial plate (NP), lower lip (LL) with lower labial projections (LP), labial papillae on the free border of the lip (red arrowheads), lower incisive teeth (IN), nostrils (NO), oral commissure (RC), and cheek (CH)

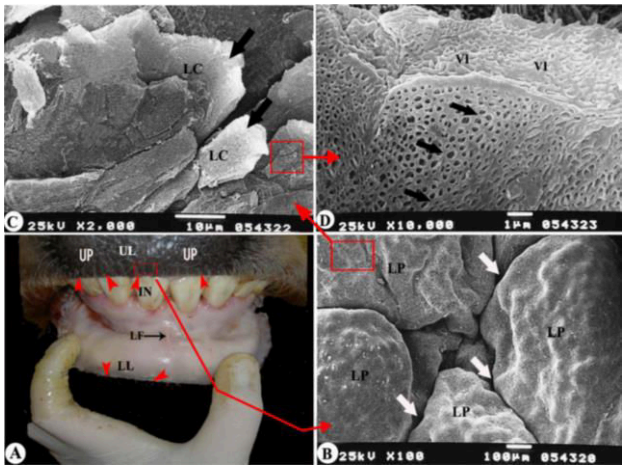

Fig. 2: Gross anatomical image (**A**) and SEM images (**B**, **C**, and **D**) of the lips of the Egyptian water buffalo. (**A**) Shows the upper lip (UL) with projections (UP), and nasolabial palate (NP), lower lip (LL), labial papillae on the free border of the lip (red arrowheads), lower incisive teeth (IN), and labial fissure (LF), (**B**) Shows the free border of lips showing blunt papillae (LP), and grooves between the papillae (white arrows), (**C**) Shows the higher magnifications of (**B**) free border of lips showing the exfoliation scales of the keratinized epithelium (black arrows, LC), and (**D**) represents the higher magnifications of (**C**) free border of lips showing numerous micro-ridges on the cell surface (black arrows) and papillary projections (VI)

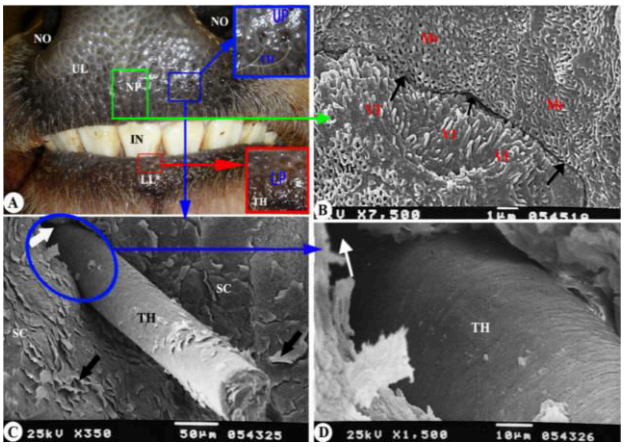

Fig. 3: Gross anatomical image (**A**) and SEM images (**B**, **C**, and **D**) of the lips of the Egyptian water buffalo. (**A**) Shows the upper lip (UL) with upper labial projections (UP), lower lip (LL) with upper labial projections (UP), tactile hair (TH), lower incisive teeth (IN), and nostrils (NO), (**B**) Represents the SEM magnification of the nasolabial plate of the upper lip to show minute papillae (VI), and micro-ridges (Mr), and grooves in between (black arrows), and (**C** and **D**) Represent the SEM of the lip showing depression (white arrow) at the origin tactile hair (TH), and scales (SC, black arrows)

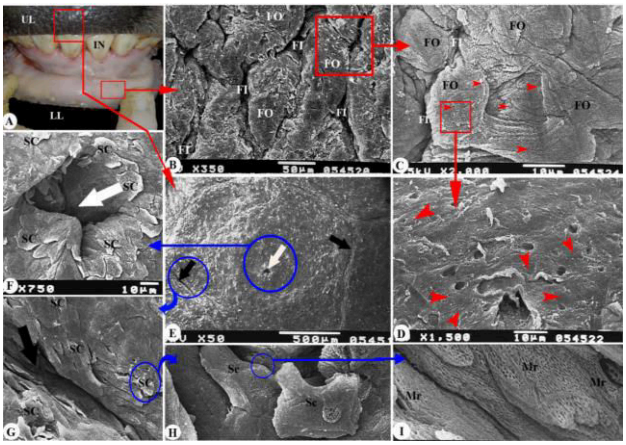

Fig. 4: Gross anatomical image (**A**) and SEM images (**B-I**) of the lips of the Egyptian water buffalo. (**A**) Shows the upper lip (UL), lower lip (LL), and lower incisive teeth (IN), (**B**, **C**, and **D**) Represent the SEM of the labial mucous membrane to show the folds (FO) and depressions in between the folds plate (FI), and the opening of labial glands (red arrowheads), and (**E-I**) Represent the SEM of the nasolabial plate to show the mucous membrane having polyhedral areas that bordered by shallow circular groove (black arrows) and contain the opening of nasolabial glands (white arrow) surrounded by numerous labial scales (SC), and micro-ridges (Mr)

magnification, each papilla had a keratinized epithelium in the form of different sized scales (Fig. 2C). With more magnification, the surface of these scales had numerous micro-ridges with small-sized papillary-like projections (Fig. 2D).

The external surface of the free movable rostral border of the upper and lower lips had numerous slightly projected labial round projections with tactile hairs (Fig. 3A). Moreover, rounded labial projection is separated by

the circular narrow, and shallow groove with SEM magnification. Each of the projected labial projections had numerous labial scales with high SEM magnifications and appeared to have numerous papillary-like projections with anastomosed micro-ridges (Fig. 3B/VI). The tactile hair had cylindrical-shaped carrying scales of keratinized stratified squamous epithelium (Figs. 3C-D).

The mucous membrane of the lips had numerous mucosal folds and depressions with scales. By magnification, the mucosal folds carried numerous openings of the labial glands of different sizes (Figs. 4A-D).

In the SEM observations, the planum nasolabial (nasolabial plate) surface had hexagonal-shaped areas separated by narrow grooves surrounded by the scale surface (Fig. 4A). The central area of each hexagonal-shaped area had a small, rounded opening of the nasolabial gland (Fig. 4E). By a high magnification, the opening of the nasolabial gland had an irregular border that carried numerous scales (Figs. 4E-F). The nasolabial plate surface carried numerous scales of keratinized epithelium that with high magnification appeared to have numerous micro-ridges and minute labial papillae on the cell's surface (Figs. 4G-I).

Histological observations of the lips and cheek

The light microscopic examination revealed that the two lips were covered externally with skin formed from the epidermis and dermis. The epidermis was covered with keratinized stratified squamous epithelium. The dermis was a dense irregular connective tissue containing hair follicles and sebaceous glands. The epidermis formed epidermal pegs interdigitated with the dermal papillae (Figs. 5A-B). The internal surface of the lips was lined with a keratinized stratified squamous epithelium. Under this epithelium, there was the propria-submucosa of the dense irregular connective tissue. The cores of lips had skeletal muscles separated with the connective tissue (Figs. 5A-D).

The external and internal surfaces of the free border of the nasolabial plate were covered with the keratinized stratified squamous epithelium (Figs. 5A-B). The degree of keratinization was more on the external surface than the internal one. The connective tissue under the two epithelium surfaces was highly vascular and contained lobules of serous glands (Figs. 5C-D). These lobules were separated with connective tissue septa. There were some bundles of skeletal muscles observed (Figs. 5C-D).

The mucocutaneous junctions of the lips revealed that they covered stratified squamous keratinized epithelium (Fig. 6A). Also, the labial mucous membrane is covered with a stratified squamous thick keratinized epithelium. Under it, there is the lamina propria layer containing the collagen fibers clear with Van Giessen stain (Fig. 6B).

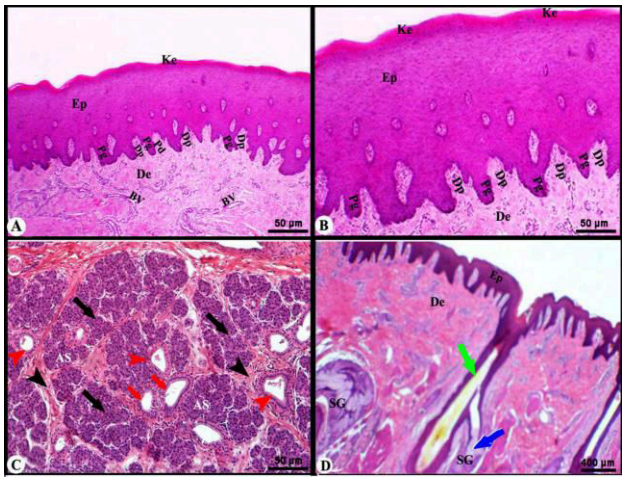

Fig. 5: Micrographs images of the lips of the Egyptian water buffalo. (**A**-**D**) Represent the cross-section of the nasolabial plate of the upper lip to show keratinized material (Ke) covering the stratified squamous epithelium (EP), epidermal peg (Pg), dermal papillae (Dp), dermis (De), blood vessels (BV), striated duct (acidophilic) of labial glands (red arrowheads), acini (AS, black arrow) with striated duct (white arrows), connective tissue septae (black arrowheads), and interlobular ducts (red arrowheads), the hair follicle (green arrows) and sebaceous glands (SG, blue arrow), (H&E, ×40) (**A**-**C**), and ×4 (**D**)

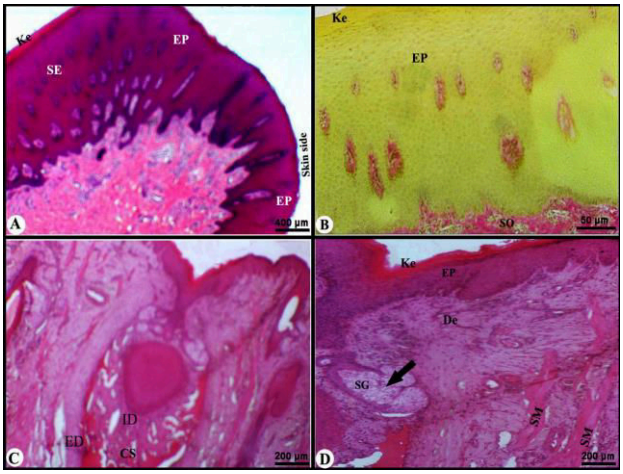

Fig. 6: Micrographs images of the lips of the Egyptian water buffalo. (**A**) Represents the mucocutaneous junction of the lip to show keratinized material (Ke) covering the stratified squamous (SE) epithelium (EP), (H&E, ×4), (**B**) Represents the labial mucous membrane to show keratinized material (Ke) covering the stratified squamous epithelium (EP), submucosa (SO), (Van Gieseon, ×40), (**C**) Represents the tactile hair to show internal dermal sheath (ID), external dermal sheath (ED), and cavernous type sinus (CS), (H&E, ×10), and (**D**) Represents the tactile hair to show keratinized material (Ke) covering the stratified squamous epithelium (EP), dermis (De), and sebaceous glands with the hair (black arrow), and skeletal muscle (MS), (H&E, ×10)

Two types of hair follicles were observed in the dermis of the covering skin: the normal (single hair follicle) and cavernous types. The cavernous type is characterized by the cavernous space between the external and internal dermal root sheaths. These cavernous spaces are formed from irregular blood spaces lined with endothelial cells. These blood spaces are separated by connective tissue trabeculae aroused from

the external and internal dermal root sheaths (Figs. 6C-D and 7A-C).

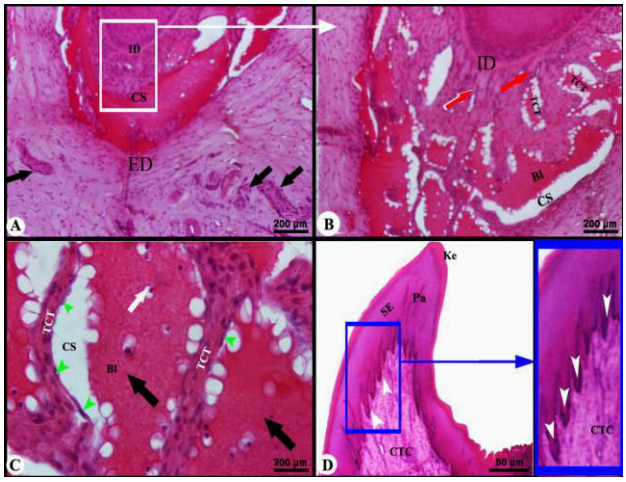

Fig. 7: Micrographs images of the lips of the Egyptian water buffalo. (**A**, **B**, and **C**) Represent the tactile hair to show internal dermal sheath (ID), external dermal sheath (ED), endothelial cells (green arrowheads) that cover cavernous sinus (CS), trabeculae connective tissue (TCT, red arrow), nerve fibers associated with hair (yellow arrows), hemolysis RBCs (Bl, black arrow), and leukocyte (white arrow), (H&E, ×10), and (**D**) Represents the labial commissure to show caudally directed conical-shaped papillae (Pa) covered with keratinized material (Ke) covering the stratified squamous epithelium (SE), primary connective tissue core (CTC), and epidermal peg (white arrowheads), (H&E, ×40)

The oral commissure had conical papillae projected from the mucous membrane. Each papilla had a papillary core of the highly vascularized connective tissue. The keratinized epidermal layer is thicker at the rostral part of the papillae than the caudal part (Fig. 7D). At the rostral part, the connective tissue papillae are more than that observed at the caudal part (Fig. 7D). The epidermal pegs were projected into the connective tissue core (Fig. 7D/white arrowheads). At the same time, the external aspect of the oral commissure consisted of a thin skin with a hair follicle and sebaceous glands. The oral commissure core consisted of skeletal muscles bundles arranged mainly longitudinally. The Seromuoid glands were occasionally observed under the mucous membrane of the oral commissure in which these glands gave a positive reaction for PAS and AB (Fig. 8).

Cheek

Gross and SEM morphological appearance of the cheek

Grossly, the cheek is attached to the alveolar margin of the maxilla and mandible and extended from the angle of the mouth rostrally to the pterygomandibular fold caudally (Figs. 9A-B). The cheek consisted of three layers: skin externally, muscular, and glandular layer in the middle, and mucous membrane internally. The external surface of the cheek was thick and covered by ordinary and tactile hairs (Fig. 1B). The inner layer of the cheek formed wide extensive mucous membrane attached ventrally to the alveolar border of the mandible from the corner of the mouth rostrally to the level caudal to the maxillary tuber caudally, in addition, it continued with the gum mucous membrane (Figs. 9A-B). It attached caudally to the alveolar border of the maxilla from the level of oral labial commissure to the maxillary tuber; it came along with the gum mucous membrane around the upper cheek teeth and with the mucous membrane of the hard palate around the inter-dental space (Fig. 9B).

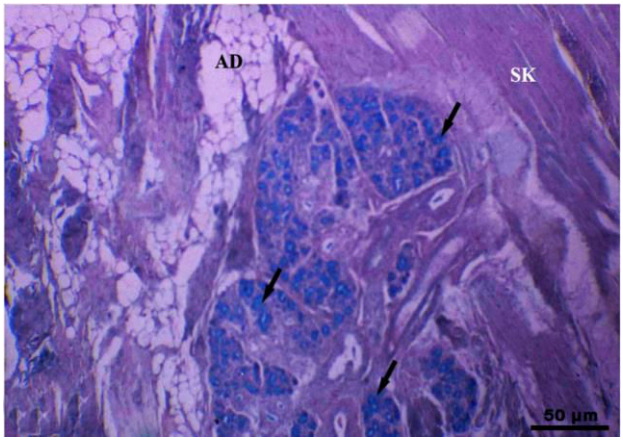

Fig. 8: Micrograph images of the labial glands of the Egyptian water buffalo to show the mixed labial glands with some lobules react positively with AB (black arrows), skeletal muscles (SK), and adipose tissue (AD), (Ab 2.5, ×40)

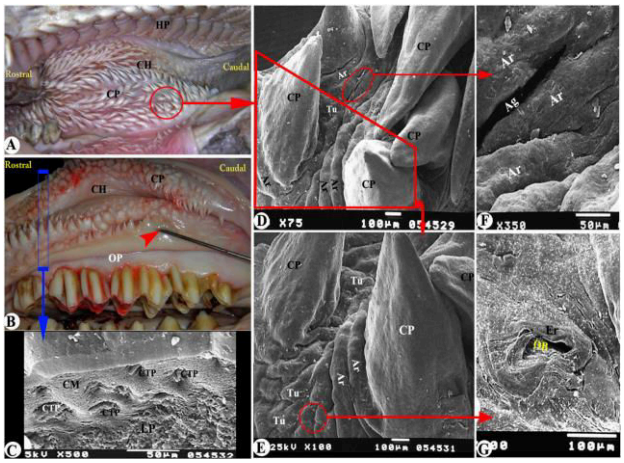

Fig. 9: Gross anatomical images (**A** and **B**) and SEM images (**C**-**G**) of the inner cheek surface of the Egyptian water buffalo. (**A** and **B**) Represent the gross image of the mucous membrane of the cheek (CH) to show the conical PAPILLAE (CP), hard palate (HP), and the opening of the parotid duct (red arrowheads), (**C**) Represents the SEM cross-section in the cheek to show the mucosa of cheek (CM), lamina propria (LP), and connective tissue papillae (CTP), and (**D**-**G**) Represent the SEM of the mucous membrane of the cheek to show the conical papillae (CP), annular folds (Ar) separated by an annular groove (Ag), elevated tubercle (Tu), the opening of buccal glands (OR), and elevated ridge (Er)

By SEM observations, the inner surface of the mucous membrane was studded with numerous conical papillae arranged in 12-14 transverse papillary rows in

the rostral part of the cheek (Figs. 9D-E). The density of the conical papillae had some variations along the whole length of the mucous membrane as the following: the rostral part contains a large number of the large-sized caudally directed conical papillae. In contrast, the dorsal part contains numerous conical papillae than the ventral part. There was a smaller number of conical papillae in the caudal part that focused caudodorsally and caudoventrally. In contrast, the middle part was devoid of the conical papillae but contained few short, blunted papillae in which some were branched. The conical papillae had different directions and were separated by interpapillary space containing numerous small, elevated tubercles and ridges with microgrooves in between. In addition, each papilla was surrounded by 2 or 3 annular ridges (Figs. 9D-F). The interpapillary space had a small opening of the buccal glands that bordered by an elevated ridge (Figs. 9E-G/OB, Er).

The opening of the parotid duct was observed in the buccal vestibule as a slit-like opening at the level of the upper 4th cheek tooth (Fig. 9B/red arrowheads). Our observation revealed that there were not any parotid papillae in the cheek of buffalo. The opening of the parotid duct was directed longitudinally. The mucosal surface had numerous depressions that indicated the site of the connective tissue papillae of epithelium, and the submucosal was somewhat loose (Fig. 9C).

Histological observations of the lips and cheek

The cheek structure was similar to that of the lip, skin externally, and mucus membrane internally with the core of skeletal muscle. The mucus membrane was keratinized stratified squamous epithelium. The epidermis formed epidermal pegs interdigitated with the dermal papillae (Figs. 10A-B). Conical papillae projected from the mucus membrane and directed caudally (Figs. 10A-B). The conical papillae had two surfaces. The rostral surface was highly keratinized than the caudal one. The core of the conical papilla contained primary connective tissue papilla, projected from it secondary connective tissue papillae into the epithelium. The keratinization and secondary connective tissue papillae numbers in the rostral surface were more than in the caudal surface (Figs. 10C-D).

The core of the cheek was formed of skeletal muscle and buccal glands. The buccal gland was compound tubuloacinar mixed (mucoserous) gland. The gland is composed of several lobules separated by connective tissue septa. The mucus acini only reacted to PAS and AB (Fig. 10C).

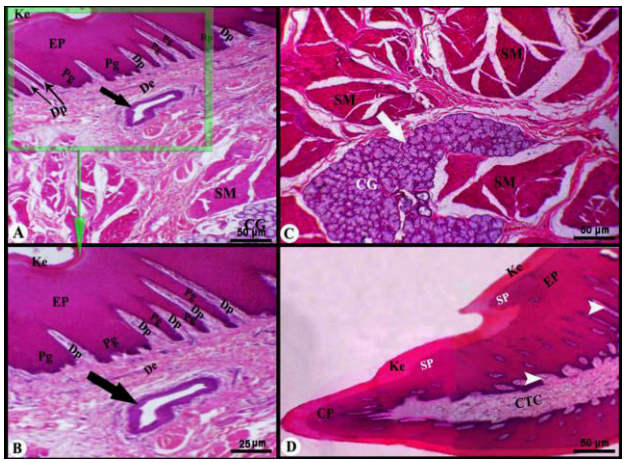

Fig. 10: Morphological images (**A**, **B**, **C**, and **D**) of the cheek of the Egyptian water buffalo to show the keratinized layer (Ke) covering the cheek mucosa (EP), dermis (De), duct of the buccal glands (black arrow), epidermal peg (Pg), dermal papillae (Dp), skeletal muscle (Ms), buccal glands (white arrow, CG), conical papillae (CP), secondary conical papillae (SP), and secondary connective tissue papillae (white arrowheads), (H&E, ×40)

Hard palate

Gross anatomical observations

The mucous membrane of the hard palate was bounded by the upper dental arch and dental pad rostrally and continuous with the gums laterally, and soft palate caudally. The mucous membrane of the hard palate supported by the palatine processes of maxillae and incisive bone in addition to the horizontal lamina of the palatine bone (Figs. 11A-C and 12A-B). The width of the

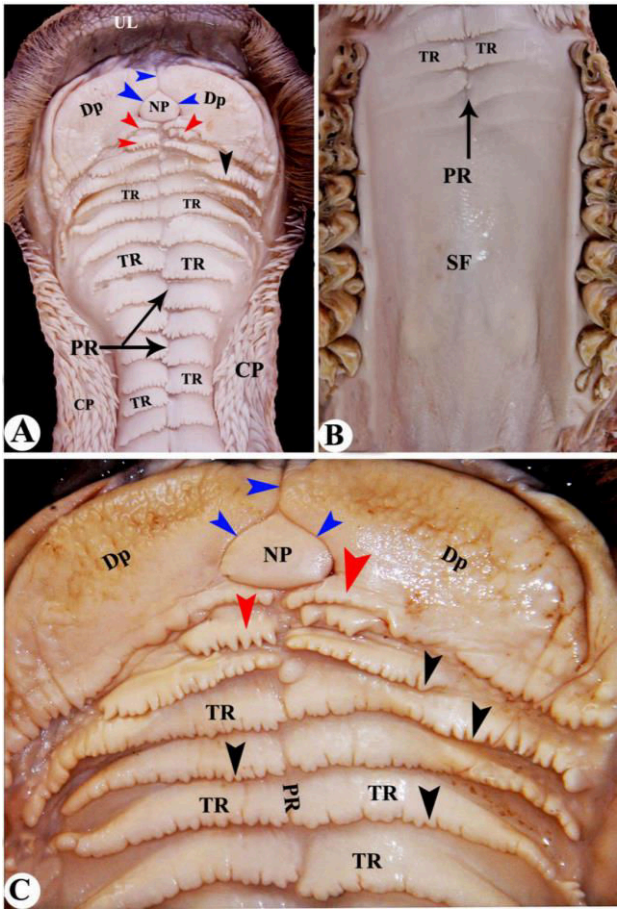

Fig. 11: Gross anatomical images of the hard palate of the Egyptian water buffalo (**A**, **B**, and **C**) to show the upper lip (UL), dental pad (Dp), and incisive papillae (NP) surrounded by a groove (blue arrowheads), four half-transverse palatine ridges that carried accessory papillae (red arrowheads), transverse ridge (TR) ended by papillae (black arrowheads), palatine raphae (PR), conical papillae (CP), and soft palate (SF)

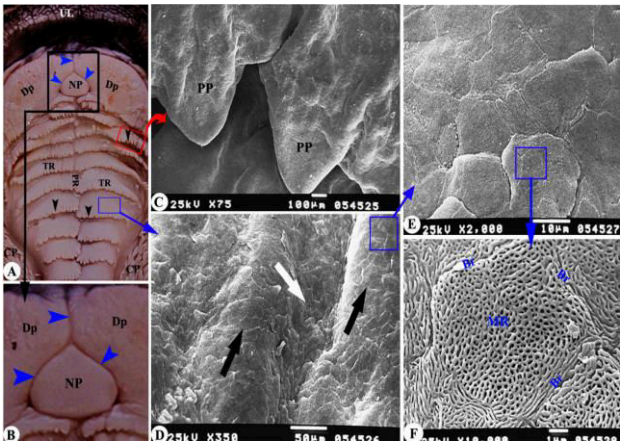

Fig. 12: Gross anatomical images (**A**-**B**) and SEM (**C**-**F**) of the hard palate of the Egyptian water buffalo. (**A**-**B**) Show the upper lip (UL), dental pad (Dp), incisive papillae (NP) surrounded by a groove (blue arrowheads), accessory papillae (red arrowheads), transverse ridge (TR) ended by papillae (black arrowheads), palatine raphae (PR), conical papillae (CP), and soft palate (SF), (**C**) Shows palatine papillae (PP), while (**D**) shows the palatine folds (black arrow) separated by depressions (white arrow), and (**E**) shows exfoliation of keratinized stratified squamous epithelium, and (**F**) showing the micro-ridges (Mr) with border (Br) on the cell surface

hard palate varies according to the region. It was bottle-shaped, wide at the rostral and caudal part, narrow in the middle of the level of interdental space. The length of the hard palate measured about 29 cm from the incisive papillae to the beginning of the soft palate, while it reached 31 cm in length from the dental pad till the beginning of the soft palate.

The hard palate is divided into two halves by a median palatine raphe that appeared as a shallow groove from which a series of palatine ridges (rugae palatini) arises. The palatine ridges on each side of the palatine raphae varied from one side to another. It was 18 on the right side and 19 on the left side. The caudally directed palatine ridges presented only on the rostral half of the hard palate. The caudally directed palatine ridges were concave in shape and carried cornified papillae on their free border. It was faded out at the level of the first cheek teeth. Caudal to the first cheek teeth, the hard palate was smooth, concave, and contained numerous palatine glands. Just caudal to the dental pad, four half-transverse palatine ridges (two on each side) carried the caudally directed accessory papillae (Figs. 11 and 12A-B).

The upper incisors were replaced by the highly keratinized dental pad (*Pulvinus dentalis*) that appeared as a semilunar area divided by the presence of the incisive papillae into two equal halves (right and left) (Figs. 11A, C, and 12A-B/Dp and NP). The incisive papilla was triangular in outline and located just caudal to the central part of the dental pad (Figs. 11A, C, and 12A-B/Dp and NP). The incisive papilla was surrounded by a groove from which a central groove passes rostrally to the dental pad (Figs. 11A, C, and 12A-B/NP, blue arrowheads).

SEM observations

The palatine ridges terminated with numerous caudally directed palatine papillae, and each papilla had a rounded or pointed end and carried some elevated tubercles (Fig. 12C/PP). The oral surface of the hard palate was uneven as it carried ridges and depression in which the ridges were alternative with depressions (Fig. 12D). By high magnification, the surface of the rugae palatini carried scales due to exfoliation of the keratinized epithelium, even more with higher magnifications, there are numerous pentagonal, or a hexagonal area bordered by the slightly elevated border, and each area was studded with numerous microridges that crossed with each other forming microridges network (Figs. 12E-F).

Histological observations

The mucous membrane of the hard palate was lined by highly keratinized stratified squamous epithelium, followed by vascular dense irregular connective tissue and adipose connective tissue (Figs. 13 and 14). The rostral part of the mucous membrane of the hard palate was thrown into longitudinal folds of the rugae palatine (Fig. 13A). The oral surface of the rugae was covered with a highly keratinized epithelium than the aboral surface (Fig. 14D). The middle layers not contained palatine rugae and were smooth, covered with the stratified squamous keratinized epithelium (Figs. 13B-C, and 14A-C).

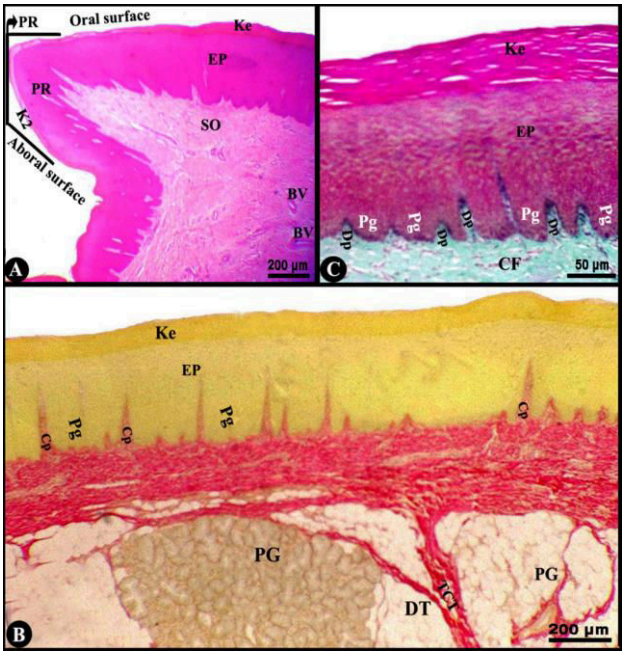

Fig. 13: Micrographs images of the papillary part (**A**-**B**) and the smooth part (**C**) of the hard palate of the Egyptian water buffalo to show the keratinized layer (Ke) covering the oral surface, (K2) the aboral surface, the stratified squamous epithelium (EP), submucosa (SO), blood vessels (BV), palatine glands (PG) with its duct (Dg), adipose tissue (DT), palatine rugae (PR), epidermal peg (Pg), dermal papillae (Dp), connective tissue (CF), connective tissue trabeculae (TCT), connective tissue papillae (Cp), (H&E, ×40) (**A**), (Van Gieson, ×40) (**B**) ×40, (H&E, ×100) (**C**)

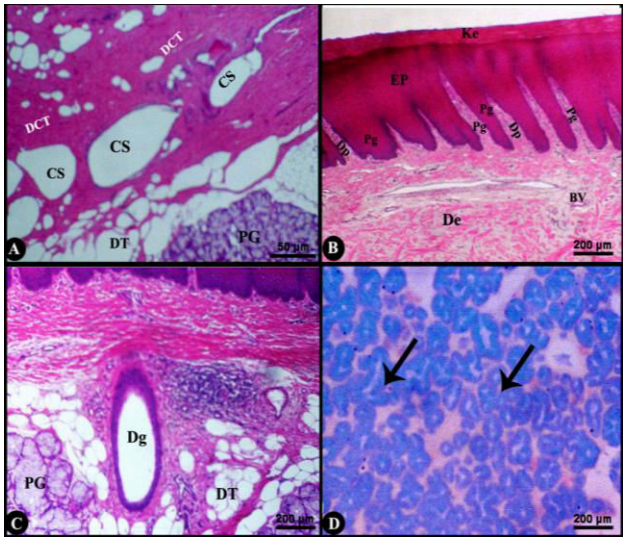

Fig. 14: Micrographs images of the hard palate of the Egyptian water buffalo. (**A-C**) the keratinized layer (Ke), the stratified squamous epithelium (EP), epidermal peg (Pg), dermal papillae (Dp), palatine glands (PG) with its duct (Dg), adipose tissue (CF), Cavernous space (CS), dense connective tissue (DCT), blood vessels (BV), and adipose tissue (DT), (H&E, ×40) (**A**), (H&E, ×100) (**B** and **C**), and (**D**) Represents the (AB) positive reaction (black arrow), (AB 2.5%, ×100)

The propria-submucosa was dense irregular connective tissue, contained compound tubuloacinar mucoserous glands. These glands had ducts opened on the surface of the hard palate. These glands showed PAS, and AB positive acini. The uppermost layer of the hard palate contained several blood vessels and venous sinuses.

The dental pads were composed of mucus membrane and propria-submucosa under it. The mucus membrane was highly keratinized stratified squamous epithelium. The degree of keratinization in the epithelium of the dental pad was the highest in the oral cavity. The propria-submucosa was dense irregular connective tissue projected several connective tissue papillae into the epithelium separated by epithelial pegs. The collagen fibers were arranged in thick bundles in different directions separated by fibroblastic connective tissue (Figs. 15A-C).

Discussion

The current work aimed to describe the gross, SEM, histological, and histochemistry features of the lips, cheek, and the hard palate of the Egyptian water buffalo. Analogous with previously published data (Dyce *et al*., 2010; Mahdy *et al*., 2020; Madkour and Mohammed, 2021), the wide large upper lip was more. This data was confirmed by the current morphometric analysis of each lip in which the upper lip (300.32 ± 5.4 ml) was longer than the lower lip (300.32 ± 5.4 ml). These observations were in compliance with that reported in the Rahmani sheep (148.79.32 ± 6.50 ml long) (Madkour and Mohammed, 2021) and goat (107.68 ± 9.08 ml long) (Mahdy *et al*., 2020).

The physiological importance of the lips aid in the process of selection, collection, and prehension of foods, as well as the suckling in the foal (Dyce *et al*., 2010). The difference in the species is in the shape and motility between the animal's species in which the motility of the upper lip is more than the lower lip (Nickel *et al*., 1986). The current observation of the mobile feature of buffalo's lips agrees with the previously published data in other ruminants' species (Getty, 1975; Nickel *et al*., 1986; Dyce *et al*., 2010; Mahdy *et al*., 2020). The current work confirmed that the movable upper lip allows ruminants, such as buffalo, to select the chosen plant

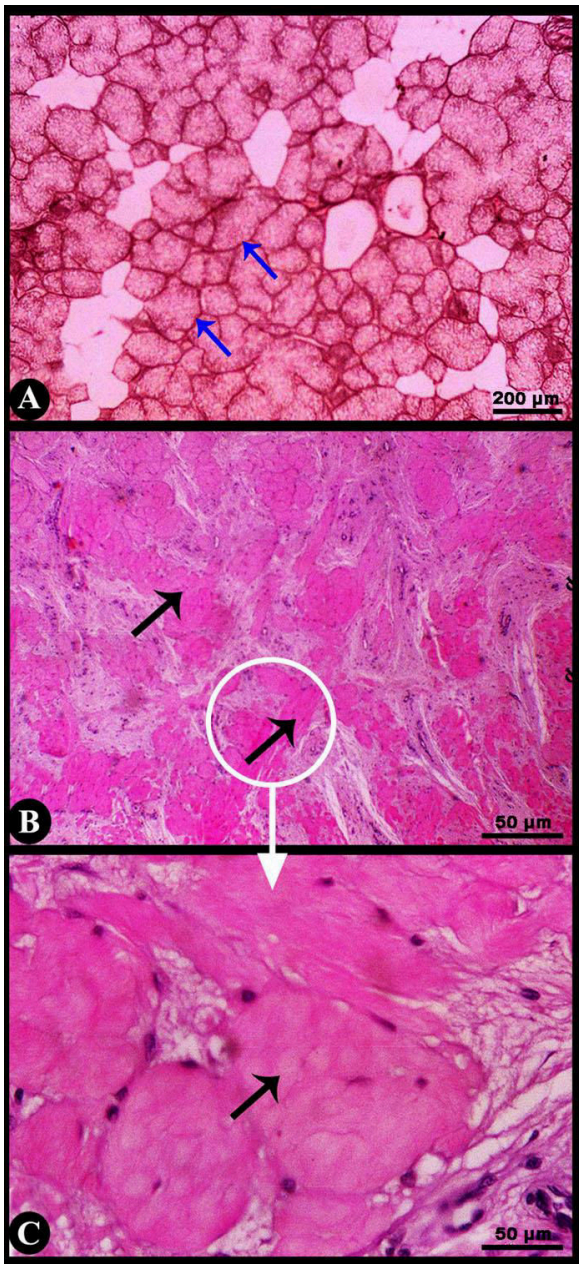

Fig. 15: Micrograph of the dental pad of the Egyptian water buffalo. (**A**) Represents the hard palate to show the elastic fibers surrounded the acini of the palatine glands (blue arrows), (Gomory, ×100), and (**B** and **C**) Represent the dental pad to show the dense regular connective tissue (black arrows), (H&E, ×40)

food particles (leaves and stems) that supply protein, energy, and minerals than the other parts of plants (Sinn and Rudenberg, 2008; Mahdy *et al*., 2020; Madkour and Mohammed, 2021).

Identical to former reports, numerous tactile hairs on the upper and lower lips surrounded the oral cleft but were absent on the oral commissure (Dyce *et al*., 2010). Furthermore, the current findings clarify the diversity of the tactile hairs in their number, length, and distribution on upper and lower lips. These findings confirmed the role of the lips as a tactile organ (Nickel *et al*., 1986; Mahdy *et al*., 2020; Madkour and Mohammed, 2021). The tactile lips of goat help to prevent the ingestion of harmful materials during nutrition (Berman *et al*., 2019). The tactile hairs of cattle are located laterally on the upper lip (Yildiz *et al*., 2004). In the current work, two types of hair follicles were observed in the dermis of the covering skin: the ordinary and cavernous types in which the cavernous type had a cavernous space between the external and internal dermal sheaths. In addition to these cavernous, the spaces formed from the anastomosed connective tissue trabeculae that arise from the external and internal dermal sheaths. The cavernous type of the tactile hairs were observed in horses (Von Rotz and Friess, 1995), sheep and cattle (Yildiz *et al*., 2004), and sheep (Madkour and Mohammed, 2021), while the sinus type was observed in cats, dogs, and rodents (Gasse and Schwarz, 2000; Ebara *et al*., 2002).

The current work reported that the free movable rostral border of the upper and lower lips carried numerous blunt short papillae separated by narrow fissures that crossed each other and carried different keratinized scales with more magnification. The surface of these scales had numerous micro-ridges with small-sized papillary-like projections. Moreover, the current work reported that the external surface of the free movable rostral border of the upper and lower lips had numerous slightly projected around labial projections with tactile hairs. The labial projections were previously recorded in domesticated ruminants (Getty, 1975; Nickel *et al*., 1986; Madkour and Mohammed, 2021). The current study observed that the labial papillae were extended to the orbicularis angles muscle and on the cheek mucous membrane; similar observations were recorded by (Nickel *et al*., 1986; Mahdy *et al*., 2020; Madkour and Mohammed, 2021), while in goats, these labial papillae are present in the buccal vestibule and absent in the labial vestibule (Sarma *et al*., 2012). Functionally, the present observations suggested that the labial projections might aid in forage selection and fixing leaves to nip them from the plant. The labial papillae help in orientating the food particles caudally toward the buccal cavity. The current SEM study reported the circular narrow and shallow groove separated the rounded labial projection. Each projected labial projection had numerous labial scales and appeared numerous papillary-like projections with anastomosed micro-ridges in high SEM magnifications. The goat (Mahdy *et al*., 2020) described the rounded labial projections on the upper lip but the pyramidal projections observed on the lower lip.

The current work observed that the mucous membrane of the lips had numerous mucosal folds and depressions with scales. In addition to SEM magnification, the mucosal folds carried numerous openings of the labial glands of different sizes. The mucosal folds and labial glands are also reported in goats (Mahdy *et al*., 2020), and sheep (Madkour and Mohammed, 2021), but the current work added that these mucosal folds carried micro-ridges. In the current work, the planum nasolabial had hexagonal-shaped areas separated by narrow grooves surrounded by the scale surface. The central area of each hexagonal-shaped area had a small, rounded opening of the nasolabial gland. The nasolabial plate surface carried numerous scales of keratinized epithelium that in high magnification, showed numerous micro-ridges and minute labial papillae on the cell's surface. The same arrangement was reported in cattle (Getty, 1975).

The cheek lining mucous membrane in all domestic animals is smooth except in ruminants possessing numerous conical papillae (Getty, 1975; Nickel *et al*., 1986; Dyce *et al*., 2010; Sarma *et al*., 2012; Pérez *et al*., 2012, 2017; Mahdy *et al*., 2020). The arrangement of the cheek conical papillae in the longitudinal rows is also recorded in alpaca (Gozdziewska-Harłajczuk *et al*., 2015), and large and small domesticated ruminants (Nickel *et al*., 1986; Dyce *et al*., 2010; Mahdy *et al*., 2020). In goat (Mahdy *et al*., 2020), the cheek papillae are represented only by the rounded shape in the third caudal part, while it is absent in the most caudal part of the cheek. The conical papillae of the cheek has an important role in the inhibition of the loss of coarse food particles during chewing process with the aid of the lips (Nickel *et al*., 1986) and maintain the cud during rumination with wide lateral movements of the jaws (Budras *et al*., 2003). Moreover, the caudal directed conical papillae, in the cheek papillae, aids the process of the food particles direction toward the pharyngeal cavity and helps the mechanical protection of the inner surface of the cheek (Gozdziewska-Harłajczuk *et al*., 2015; Mahdy *et al*., 2020). Furthermore, these large cheek papillae in ruminants provide mechanical protection for the mucous membrane against hard dry coarse foods (Masuko *et al*., 2007; Gozdziewska-Harłajczuk *et al*., 2015; Mahdy *et al*., 2020). The observations of numerous longitudinal papillary rows in buffalo confirmed the high mechanical protection of the oral cavity. This current suggestion was confirmed by the stratified keratinized epithelium of the mucous membrane.

The opening of the parotid duct of buffalo was observed in the buccal vestibule without parotid papillae in the cheek of the buffalo. The parotid duct's opening on the buccal vestibule's inner surface was observed in the goat but with parotid papillae (Mahdy *et al*., 2020). The position of the opening of the parotid duct had some variations among animal's species; the current work reported the opening at the level of the upper 4th cheek, while it is located at the level of 1st upper molar tooth in

goat (Tadjalli *et al*., 2002), at the level of upper 2nd molar tooth as observed by Nickel *et al*. (1986), Dehghani *et al*. (1994), and Budras *et al*. (2003) in buffalo and ox, Sarma *et al*. (2012) in bakerwali goats, Dehghani *et al*. (2000) in sheep. Moreover, there are some species variations in the shape of the opening of the parotid duct, which is observed as a slit-like opening in the current work, while it emerges as a rosette-shape in cattle and goats (Dehghani *et al*., 1994; Tadjalli *et al*., 2002). In goats, the parotid duct appears the elongated raised opening which bounded rostrally by conical papillae (Mahdy *et al*., 2020).

The current histological observations described that, the two lips were covered externally with the thin skin, hair follicles, and sebaceous glands and lined internally with mucous membrane. This mucous membrane consisted of stratified squamous keratinized epithelium supported by a dense connective tissue lamina propria. The same histological findings were reported by Nickel *et al*. (1986), and Saxena *et al*. (2007). Moreover, the current work observed the seromucous labial glands in goats (Habata *et al*., 2012; Mahdy *et al*., 2020) and sheep (Madkour and Mohammed, 2021). Physiologically, the labial glands may have a remarkable role in the mucosal immune system, the same results recorded in goats and sheep (Habata *et al*., 2012; Mahdy *et al*., 2020; Madkour and Mohammed, 2021). In the current observation, the buccal salivary glands were mixed (seromucous) and consisted of lobules surrounded by connective tissue fibers. Moreover, the reactivity of the glands for PAS and AB was restricted to the peripheral mucous part of the acini, but not to the center and the serous parts.

The appearance of the hard palate shows some morphological differences among animal species. The current work divided the bottle-shaped hard palate into wide rostral and caudal parts, and a narrow middle part. The hard palate appeared flat rostrally and caudally but nearly concave at its middle part (Maala *et al*., 2007). While the hard palate of the goat is described as a narrow rostral and wide caudal part (Mahdy *et al*., 2018), while Nickel *et al*. (1986) observed that the goat hard palate was uniform gradually widen at caudal, while in another report, the hard palate was found narrow rostrally and narrower at the middle, and widen at its caudal part (Sarma *et al*., 2012) in bakerwali goats. Encarnacion *et al*. (2015) also clarified that the hard palates of sheep and goat are the narrowest at the middle and wider at the caudal parts.

The current work reported that the mucous membrane of the hard palate was bounded by the upper dental arch rostrally and laterally, and continuous with the gums laterally, soft palate caudally, the dental pad rostrally, similar to that reported in cattle (Maala *et al*., 2007). The hard palate is divided into two halves by median palatine raphae that appeared as a shallow groove from which a series of palatine ridges (rugae palatini) arises. The median palatine raphe is observed in cattle as a line or groove (Maala *et al*., 2007). The palatine ridges on each of the palatine raphae varied from one side to another, reaching 18 at the right and 18 at the left sides. In horse, it reached 18 transverse ridges (Budras *et al*., 2012), while in Indian buffalo (Gupta *et al*., 1987), and Philippine water buffalo (Maala and Ferriol, 2002), the number of palatine ridges are about 16 to 20. The current work on the Egyptian water buffalo clarified the presence of the four half-transverse palatine ridges (two on each side) carrying the caudally directed accessory papillae (Just caudal to the dental pad). The accessory palatine ridges were also recorded by (Gupta *et al*., 1987; Maala and Ferriol, 2002). The currently observed accessory palatine ridges had a role in raising the hard palate's qualifications to deal with food particles during the mastication process (Gupta *et al*., 1987; Maala and Ferriol, 2002).

The caudally directed palatine ridges presented only on the rostral half of the hard palate and were concave in shape and carried cornified papillae on their free borders and caudal to the first cheek teeth. The hard palate was smooth and concave and contained numerous palatine glands. The palatine ridges of cattle appeared straight and narrowed in the rostral part but slowly appeared curved and wide at the middle and caudal parts (Nickel *et al*., 1986; Maala *et al*., 2007; Dyce *et al*., 2010). The current SEM observations clarify that the surface of the rostral part of the hard palate was uneven as it carried ridges and depression. At high magnification, the surface of the rugae palatini carried scales due to exfoliation of the keratinized epithelium, even more with higher magnifications, there were numerous pentagonal, or a hexagonal area with the slightly elevated border; each area was studded with numerous micro-ridges that crossed with each other forming micro-ridges network. The current histological observations showed that the mucous membrane of the hard palate was lined by highly keratinized stratified squamous epithelium followed by a highly vascular dense irregular connective tissue.

The upper incisors were replaced by the highly keratinized dental pad (*Pulvinus dentalis*) that appeared as a semilunar area divided by the incisive papillae into two equal halves (right and left), and the caudal border of the dental pad nearly serrated. The ovoid-shaped dental pad was directed obliquely from the midline and its lateral border was pointed but the medial border was rounded (Maala *et al*., 2007). The incisive papilla was triangular in outline and presented just caudal to the central part of the dental pad. Groove surrounded this incisive papilla from which arises a central groove passes rostrally to the dental pad. In cattle, the incisive papilla appeared as diamond or triangularly-shaped (56% of cases), round (26% of cases) and irregularly-shaped (18% of cases) (Maala *et al*., 2007).

The internal labial surface and labial mucocutaneous junctions covered with stratified squamous keratinized epithelium. The seromuoid glands were occasionally observed under the oral mucous membrane of the commissure and gave positive PAS and AB. The density of conical papillae on the inner cheek surface had some variations: the rostral part had a large number of large papillae, while the dorsal part had numerous papillae than the ventral part, the caudal part had a smaller

number of papillae, while the middle part was devoid of papillae. The conical papillae had two surfaces; the rostral surface was highly keratinized than the caudal one. The buccal gland was a compound tubuloacinar mixed (mucoserous) gland and mucus acini only reacted to PAS and AB. The palatine glands showed PAS and AB positive.

Acknowledgement

The authors extend their appreciation to the Deanship of Scientific Research at King Khalid University, Saudi Arabia for funding this work through the Research Group Project under grant number (R.G.P.2/47/42).

Conflicts of interest

The authors declare no conflicts of interest.

References

Abumandour, MM (2018). Surface ultrastructural (SEM) characteristics of oropharyngeal cavity of house sparrow (*Passer domesticus*). Anat. Sci. Int., 93: 384-393.

Abumandour, MMA and El-Bakary, RMA (2013). Morphological and scanning electron microscopic studies of the tongue of the Egyptian fruit bat (*Rousettus aegyptiacus*) and their lingual adaptation for its feeding habits. Vet. Res. Commun., 37: 229-238.

Bancroft, JD; Cook, H and Turner, D (1996). *Manual of histological techniques and their diagnostic application*. 2nd Edn., Churchill Livingstone.

Bancroft, JD and Gamble, M (2008). *Theory and practice of histological techniques*. 6th Edn., China, Elsevier Health Sciences.

Baumel, JJ (1975). In: Getty, R (Ed.), *Sisson and Grossman's the anatomy of the domestic animals*. (5th Edn.), Vol. II, Philadelphia, PA, W. B. Saunders Co.

Berman, TS; Glasser, TA and Inbar, M (2019). Goats adjust their feeding behaviour to avoid the ingestion of different insect species. Can. J. Zool., 97: 805-811.

Bone, RM (1979). *Anatomy and physiology of farm animals*. 2nd Edn., Virgina, USA, Reston Publishing Co., P: 560.

Budras, KD; Habel, RE; Wunsche, A and Buda, S (2003). *Bovine anatomy: An illustrated text*. 1st Edn., Vol. 1, KG, Verlag und Druckerei, Hannover: Schlutersche GmbH & Co., PP: 34-35.

Budras, KD; Sack, WO and Röck, S (2012). *Anatomy of the horse: with Aaron Horowitz and Rolf Berg*. 6th Edn., Schluetersche. PP: 44-45.

Dehghani, SN; Lischer, CJ; Iselin, U; Kaser-Hotz, B and Auer, JA (1994). Sialography in cattle: technique and normal appearance. Vet. Radiol. Ultrasound., 35: 433-439.

Dehghani, S; Tadjalli, M and Masoumzadeh, M (2000). Sialography of sheep parotid and mandibular salivary glands. Res. Vet. Sci., 68: 3-7.

Dyce, KM; Sack, WO and Wensing, CJG (2010). *Text book of veterinary anatomy*. 5th Edn., Philadelphia, London and Toronto, W. B. Saunders Co., PP: 654-655.

Ebara, S; Kumamoto, K; Matsuura, T; Mazurkiewicz, JE and Rice, FL (2002). Similarities and differences in the innervation of mystacial vibrissal follicle-sinus complexes in the rat and cat: a confocal microscopic study. J. Comp. Neurol., 449: 103-119.

El-Bakary, NER and Abumandour, MMA (2017). Morphological studies of the tongue of the Egyptian water buffalo (*Bubalus bubalis*) and their lingual papillae adaptation for its feeding habits. Anat. Histol. Embryol., 46: 474-486.

Encarnacion, JML; Maala, CP and Ducusin, RJT (2015). Comparative gross and microscopic anatomy of the hard palate and palatine printing in goat (*capra hircus* l.) and sheep (*ovis aries* l.). Philipp. J. Vet. Med., 52: 71-82.

FAO (2013). Breeds reported by Pakistan: buffalo. Domestic Animal Diversity Information System, Food and Agriculture Organisation of the United Nations, Rome.

Gasse, H and Schwarz, R (2000). The sinus hair follicle of the cat. Cells Tissues Organs. 166: 354-358.

Getty, R (1975). *The anatomy of the domestic animals*. 5th Edn., Vol. 1, Philadelpshia, USA, W. B. Saunders Co., PP: 234-236.

Gozdziewska-Harłajczuk, K; Kleckowska-Nawrot, J; Janeczek, M and Zawadzki, M (2015). Morphology of the lingual and buccal papillae in Alpaca (*Vicugna pacos*) - Light and scanning electron microscopy. Anat. Histol. Embryol., 44: 345-360. doi: 10.1111/ahe.12147.

Gupta, SK; Sharma, DN and Bhardwaj, RL (1987). Comparative anatomy of the palate (*palatum durum*) of buffalo (*Bubalus bubalis*) and ox (*Bos indicus*). Haryana Veterinarian. 24: 22-26.

Habata, I; Yasui, T; Fujimori, O; Meyer, W and Tsukise, A (2012). Histochemical analyses of glycoconjugates and antimicrobial substances in goat labial glands. Acta Histochem., 114: 454-462.

Klein, J; Adams, S; De Moura, A; Alves Filho, D; Maidana, F; Brondani, I; Cocco, JM; Rodrigues, LDS; Pizzuti, LAD and Da Silva, M (2021). Productive performance of beef cows subjected to different nutritional levels in the third trimester of gestation. Animal. 15: 1000-1089.

König, HE and Liebich, HG (2013). *Veterinary anatomy of domestic mammals: textbook and colour atlas*. Schattauer Verlag. 4th Edn., P: 303.

Maala, CP; Ducusin, RJT and Rizon, JA (2007). The gross anatomy of the hard palate and palatine printing in cattle. Philipp. J. Vet. Med., 44: 1-7.

Maala, CP and Ferriol, GAS (2002). Gross anatomy, histology and palatine prints of the hard palate of the Philippine carabao (*Bubalus bubalis* L.). Philipp. Agric. Sci., 65: 57-67.

Madkour, FA and Mohammed, ES (2021). Histo-morphological investigations on the lips of Rahmani sheep (*Ovis aries*): A scanning electron and light microscopic study. Microsc. Res. Tech., 84: 992-1002.

Mahdy, MAA; Abdalla, KEH and Mohamed, S (2018). Morphological study of the hard palate in the Egyptian goats (*Capra hircus*): A scanning electron microscopic study. Anat. Histol. Embryol., 47: 391-397.

Mahdy, MAA; Mohamed, SA and Abdalla, KEH (2020). Morphological investigations on the lips and cheeks of the goat (*Capra hircus*): A scanning electron and light microscopic study. Microsc. Res. Tech., 83: 1095-1102.

Masson, P (1929). Some histological methods: trichrome staining and their preliminary technique. J. Tech. Methods. 12: 75-90.

Masuko, TS; Boaro, N; König-Júnior, B; Cabral, RH and Costa-Neto, JM (2007). Comparative scanning electron microscopic study of the lingual papillae in three species of bats (*Carollia perspicillata*, *Glossophaga soricin*a and *Desmodus rotundus*). Microsc. Microanal., (Suppl. 2), 13: 280-281.

Nickel, R; Schummer, A; Seiferle, E; Frewein, J; Wilkens, H and WILLE, KH (1986). *The anatomy of the domestic animals*. 1st Edn., Translation by Siller, WG and Wight, PAL, Berlin, Hamburg, Springer-Verlag Paul Parey.

Pérez, W; Michel, V; Jerbi, H and Vazquez, N (2012). Anatomy of the mouth of the giraffe (Giraffa camelopardalis rothschildi). Int. J. Morphol., 30: 322-329.

Pérez, W; Vazquez, N and Ungerfeld, R (2017). Gross anatomy of pampas deer (Ozotoceros bezoarticus, Linnaeus 1758) mouth and pharynx. Anat. Histol. Embryol., 46: 195-203.

Sarma, K; Suri, S; Devi, J and Doley, P (2012). Morphological studies on the mouth cavity of bakerwali goat (*Capra hircus*) of Jammu region. Indian J. Vet. Anat., 24: 20-21.

Saxena, V; Gupta, A and Jain, R (2007). Topographic anatomy of the buccal and labial glands in goat (*Capra hircus*). Indian J. Anim. Sci., 77: 588-589.

Schumacher, U; Duku, M; Katoh, M; Jörns, J and Krause, WJ (2004). Histochemical similarities of mucins produced by Brunner's glands and pyloric glands: A comparative study. *The Anatomical Record Part A: Discoveries in Molecular, Cellular, and Evolutionary Biology: An Official Publication of the American Association of Anatomists*. 278: 540-550.

Seeley, RR; Stephens, TD and Tate, P (2006). *Reproduction and development. Anatomy & physiology*. 7th Edn., St Louis, McGraw-Hill Publishers. P: 125.

Sinn, R and Rudenberg, PG (2008). *Raising goats for milk and meat*. 1st Edn., Heifer International.

Suvarna, SK; Layton, C and Bancroft, JD (2013). *Bancroft's theory and practice of histological techniques*. Expert Consult: Online and Print, 7: *Bancroft's theory and practice of histological techniques*. Churchill Livingstone, Churchill Livingstone Elsevier.

Suvarna, KS; Layton, C and Bancroft, JD (2018). *Bancroft's theory and practice of histological techniques*. E-Book: Elsevier Health Sciences.

Tadjalli, M; Dehghani, SN and Ghadiri, M (2002). Sialography of the goat parotid, mandibular and sublingual salivary glands. Small Rumin. Res., 44: 179-185.

Von Rotz, A and Friess, A (1995). A scanning electron-microscopic analysis of the morphology of equine lower lip sinus hair. Cells Tissues Organs. 154: 196-204.

Yildiz, D; Gultiken, M and Karahan, S (2004). The scanning electron and light microscopic structure of bovine tactile hair. Anat. Histol. Embryol., 33: 304-308.